Journal of Applied Polymer Science

Asymmetric polysulfone gas separation membranes treated by low pressure DC glow discharge plasmas

Chalad Yuenyao,[1,2] Yutthana Tirawanichakul,[1,2,3] Thawat Chittrakarn[1,3]

[1]Faculty of Science, Department of Physics, Prince of Songkla University, Hat Yai, Songkhla 90112, Thailand
[2]ThEP Center, CHE, Bangkok 10400, Thailand
[3]Faculty of Science, Membrane Science and Technology Research Center, Prince of Songkla University, Hat Yai, Songkhla 90112, Thailand
Correspondence to: T. Chittrakarn (E-mail: tawat.c@psu.ac.th) and C. Yuenyao (E-mail: chalady_2012@hotmail.com)

ABSTRACT: Asymmetric polysulfone (PSF) gas separation membranes were prepared at different conditions such as non-solvent concentration, evaporation time (ET) and coagulation bath temperature (CBT). In addition, effects of low-pressure DC glow discharge plasma on the characteristics of PSF membranes were investigated. PSF membranes both before and after plasma treatment were characterized by several techniques, including contact angle measurement, scanning electron microscope (SEM), dynamic mechanical thermal analysis (DMTA), and atomic force microscopy (AFM). Furthermore, the performance of membranes was evaluated in terms of permeability of CO_2, CH_4, O_2, and N_2 gases. The ideal selectivity of CO_2/CH_4 and O_2/N_2 and surface free energy was calculated. Results showed that the EtOH concentration, ET and CBT affect the morphology of PSF membranes. For membranes prepared from a casting solution consisting of PSF 26.0, NMP 28.0, THF 28.0, and EtOH 18.0 wt % and ET for 3 min, the maximum selectivity of untreated membrane is about 69.76 and 12.59 for CO_2/CH_4 and O_2/N_2, respectively. After plasma treatment, the ideal selectivity is receded; however, the CO_2/CH_4 is still higher than 40.41 at pressure of 5 bars. Finally, preparation conditions and DC glow discharge plasmas have significant effects on the characteristics of the PSF membranes and result in an increase of the gas permeation. © 2015 Wiley Periodicals, Inc. J. Appl. Polym. Sci. **2015**, *132*, 42116.

KEYWORDS: membranes; morphology; oil and gas; surfaces and interfaces; separation techniques

Received 3 October 2014; accepted 18 February 2015
DOI: 10.1002/app.42116

INTRODUCTION

Polysulfone (PSF) is one of the important polymeric materials used for the preparation of gas separation membranes, because it has excellent properties like high mechanical, chemical, and thermal resistance and it is easy to handle for film-forming.[1–3] Furthermore, the separation and plasticization properties of PSF are in acceptable levels.[3,4] Therefore, many research groups are intensively working on the enhancement of membranes properties and performances; mainly utilizing two types of techniques.[5]

The first technique is the modification of the membrane bulk structure by chemical processes. This technique includes the variation of preparing conditions and parameters as well as the composition of polymer solution.[6–9] For example, in 2004 Ismail and Lai[10] developed defect-free asymmetric PSF membranes for gas separation through the manipulation of membrane fabrication variables such as polymer concentration and solvent ratio. They found that the selectivity of developed membrane was relatively higher compared to conventional membranes. Besides, Ma *et al.*[11] added the polyethylene glycol (PEG) in the preparation of PSF membranes using the phase inversion method. They found that the separation performance in terms of pure water flux (PWF) increased. In 2011, Madaeni and Moradi[4] and Aroon *et al.*[12] prepared PSF gas separation membranes by varying the preparation conditions like polymer concentration, solvent and nonsolvent types, additives, components of coagulation medium, thickness of the membrane, immersion time, and coagulation bath temperature (CBT). They indicated that the performance of PSF membranes can be changed by an adjustment of the aforementioned parameters and preparing conditions. For instance, the flux of gases through prepared membranes was receded as well as the O_2 and CH_4 selectivity were improved with the increment of polymer concentration and addition of a volatile solvent in the polymer solution, respectively. Recently, the effect of preparing parameters on the morphology and performance of polydimethylsiloxane/polysulfone (PDMS/PSF) was investigated. It was found that the addition of nonsolvent additive; ethanol (EtOH), in

polymer solution can increase the CO_2/CH_4 selectivity from 25.4 (with free EtOH) to 28.8 (with 14.4 wt % EtOH). In addition, with increasing of CBT, the pore diameter and number of macro voids increased.[13,14] The effect of evaporation time (ET) on membrane properties and morphologies was also studied. It was found that the thickness of the skin layer could be controlled by the evaporation condition.[15,16] Permeability of O_2 and N_2 through polyethersulfone (PES) decreased while the O_2/N_2 selectivity increased with an increase of ET.[16,17]

The second technique that is used to further increase the gas separation performance of membranes is the modification of membrane surfaces by physical or physicochemical processes.[6,7] Glow discharge plasma at low pressure is one of the most important techniques used to modify the morphology and properties of polymeric membranes surfaces.[2,18–21] Most of glow discharge plasmas used for these aims was generated by using radio frequency (13.56 MHz) and microwave (2.45 GHz) power sources. However, comparing both techniques, glow discharge plasma from a DC power source is the easier and simpler technique. From literature it is known that glow discharge plasmas at different conditions employed increase the separation performance of polymeric membranes. For example, Pal *et al.*[21] and Kim *et al.*[22] reported that the permeation of polyethersulfone (PES) and PSF ultrafiltration membranes has improved after treated by plasmas using CO_2 and O_2 as working gases, respectively. The pore size of PSF membranes increased after treated with CO_2-plasma.[23] Also, the PSF membranes are treated with N_2-plasma at different conditions. The results show that the pore diameters became larger and the pores size distribution became wider. However, a prolonged treatment did not affect the pore size because of the balancing effect of the etching and deposition processes.[24] The surface roughness of high density polyethylene (HDPE) and low density polyethylene (LDPE) membranes increased whereas the thickness of the top skin layer decreased. Moreover, functional groups like peroxide, ester, carbonyl, carboxyl, hydroxyl, and amide, were introduced onto the top skin layer of both HDPE and LDPE membranes after Ar-plasma treatment.[25] On the other hand, the average surface roughness of PES membranes treated by CO_2-plasma declined clearly with increasing plasma treatment time.[21] In 2009, Jian *et al.*[26] reported that the size and distribution of pores on the polyvinylidene fluoride (PVDF) membrane surfaces are smaller and narrower after plasma treatment. Akishev *et al.*[27] found that the hydrophilic property of polypropylene (PP) and polyethylene terephthalate (PET) in terms of water contact angle is improved after treated with air and N_2 plasmas at atmospheric pressure. They also found that the water contact angle decreased when the plasma treatment time increased to three seconds. Lastly, PSF membrane for CO_2/CH_4 separation was modified by low frequency O_2-plasma. The permeability of plasma treated membrane increased to 5.63 and 68.80 GPU for CH_4 and CO_2, respectively, whereas, the CO_2/CH_4 selectivity varied from 7.7–45.3, depending on the treatment conditions.[3]

The first aim of this work was to study the effects of the concentration of EtOH, ET, and CBT on the structures of the resulted membranes. The second aim was to investigate the effect of DC glow discharge plasma at low pressure on the morphology and structural properties of PSF membrane surfaces using different types of working gas. Additionally, the performance of obtained membranes in terms of the permeation of CO_2, CH_4, N_2, and O_2 gases, both before and after plasma treatment were measured. Finally, the ideal gas separation factor for CO_2/CH_4 and O_2/N_2 were calculated and compared between virgin and plasma treated membranes.

EXPERIMENTAL

Materials

Pellets of PSF (UDEL P-1700) were supplied by Solvay, China. 1-Methyl-2-pyrrolidone (NMP) was supplied by Sigma-Aldrich, while Dimethylacetamide (DMAC) and tetrahydrofuran (THF) were purchased from Fluka Riedel-deHaën and Ajax Finechem Pty, respectively. Nonsolvents, including Ethanol (EtOH; C_2H_5OH, $M_w = 46.07$ g/mol, 99.5%) and methanol (MeOH; CH_3OH, $M_w = 32.04$ g/mol, 99.5%) were supplied by Merck. CH_4, CO_2, O_2, N_2, and Ar gases with purity of 99.5%, 99.5%, 99.5%, 99.995%, and 99.95%, respectively, were supplied by Linde Company (Thailand) Ltd.

Preparation of Asymmetric Flat Sheet Membranes

The pellets of PSF were dried at 85°C for 24 h before use. All of the constituents are weighed according to a given formula. Afterwards the PSF pellets were poured into the solvents and stirred with a hot plate magnetic stirrer at a temperature of about 55–60°C for 24 h or until the PSF material was completely dissolved.

In this work, the PSF membrane that is consisted of 26 wt % PSF, 28 wt % NMP, 28 wt % THF, and 18 wt % EtOH, were used for plasma treatment. The polymer solution was casted on a clear and smooth glass plate to a thickness of about 200 μm. To enhance the gas separation performance of the membranes, preparing conditions were adapted from literatures.[3,13,15] These conditions comprised of ET in the normal ambient air for 3 min and an immersion time in a double coagulation bath of deionized water at about 20°C for 15 min, and of MeOH at about 15°C for 2.5 h. After the immersion in the MeOH bath, the membranes were dried in the normal air (about 24–25°C) for 24 h and were dried in an electric oven at 60°C for 3 h before use.

Plasma Treatment of PSF Membranes

The DC-glow discharge plasma at low pressure using for treatment of PSF membranes was generated in a cylindrical vacuum chamber of 255 mm diameter and 381 mm length.[9] Samples of PSF membranes were placed on the anode electrode of 200 mm diameter as shown in Figure 1. As the temperature of the electrode may increase the membrane samples were not in direct contact to the electrode surface.

After the membrane sample was loaded, the vacuum pump was started to evacuate the base pressure down to about 0.05 mbar. Then the working gas was fed into the chamber until the pressure has reached about 0.25 mbar. In all experiments, the working gas was flown through the chamber at this pressure for about 5 min to minimize the contamination from other gases. The DC power was applied to kindle the plasma. The plasma treatment time and discharge power were controlled at about 5 min and 15

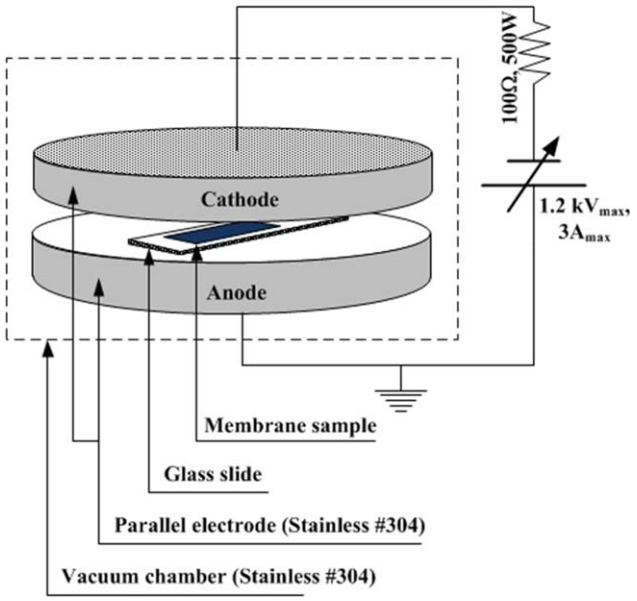

Figure 1. Placement of PSF membranes on the anode electrode during plasma treatment. [Color figure can be viewed in the online issue, which is available at wileyonlinelibrary.com.]

W, respectively. After plasma treatment, the DC power was turned off while the working gas was still flown through the chamber for 10 min to control the ambient air effects.

Characterization of PSF Membranes

The hydrophilic property of the membranes was evaluated by contact angle measurements in sessile drop mode using a video based optical contact angle measuring instrument (Model OCA 15EC, DataPhysics Instruments GmbH, Germany). For this measurement, samples of the membrane were cut into rectangular shape of about 10 mm width and 35 mm length. Afterwards, they were fixed on glass slides. Additionally, the surface free energy (SFE) as well as their components; dispersion and polar components, was analyzed by using the SCA software. The Owens-Wendt approach was utilized.[28] Contact angles of pure water and ethylene glycol were measured for this aim. Physical and mechanical properties as well as glass transition temperature of membranes were investigated by DMTA technique in tensile mode. The frequency and temperature were controlled at 1 Hz and 20–300°C, respectively. SEM micrograph and Carnoy version 2.0 software[29] were used to estimate the top skin thickness and pore size. For morphology observation by SEM, membrane sample was immersed in liquid nitrogen for 3–5 min before ruptured into smaller pieces and then coated with gold at low pressure. The AFM, Nanosurf easyscan 2 from Nanoscience (instruments), was used to study the roughness of membrane surfaces.

Gas Permeation Measurement

PSF membranes used for the gas permeation testing were cut into circular shape with a diameter of 57 mm (membrane effective area of about 17.36 cm^2). As shown in Figure 2, PSF membrane was placed in permeation cell and the rubber O-ring was used to ensure that the gas is not leak during test.

The permeation rate of pure CO_2, CH_4, O_2, and N_2 gases through the membrane samples both before and after plasma treated were measured at different pressure levels of 5, 6, 7, and 8 bars. The pressure-normalized flux value or permeance of gas was calculated by the eq. (1).[10,12,30]

$$\left(\frac{P}{l}\right) = \frac{Q}{A\Delta p} \quad (1)$$

where Q is the measured volumetric flow rate, P is permeability, l is the skin (selective) layer thickness, A is the membrane effective area, and Δp is the pressure difference across the membrane. The unit of permeance is GPU while 1 GPU is equal to 10^{-6} cm^3 (STP)/cm^2 s cm Hg.

In addition to the pressure normalized flux value, the ideal gas separation factor ($\propto_{ij}$) or the O_2/N_2 and CO_2/CH_4 selectivity was estimated by eq. (2).[30,31]

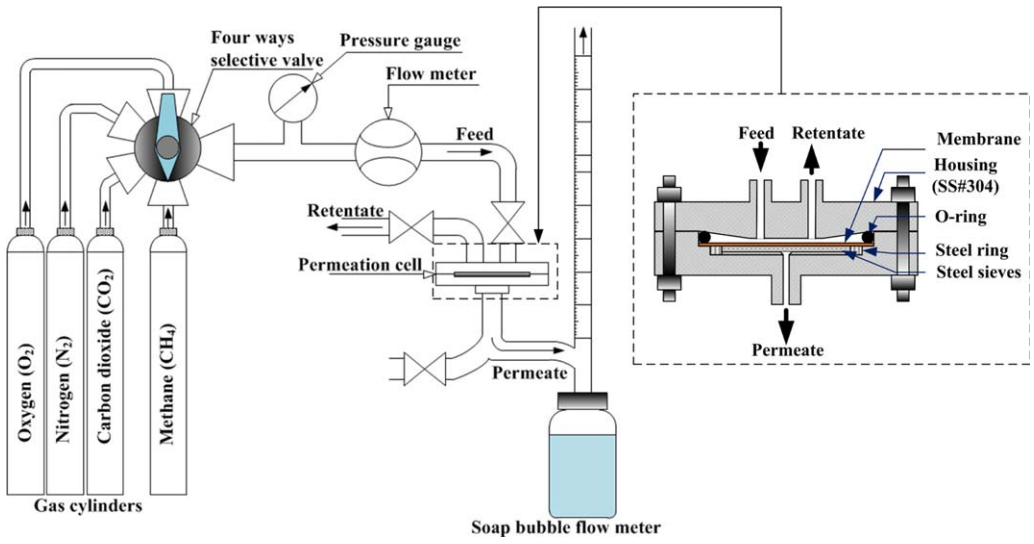

Figure 2. Schematic diagram of the gas permeation testing set, with gas cylinders, soap bubble flow meter and permeation cell. [Color figure can be viewed in the online issue, which is available at wileyonlinelibrary.com.]

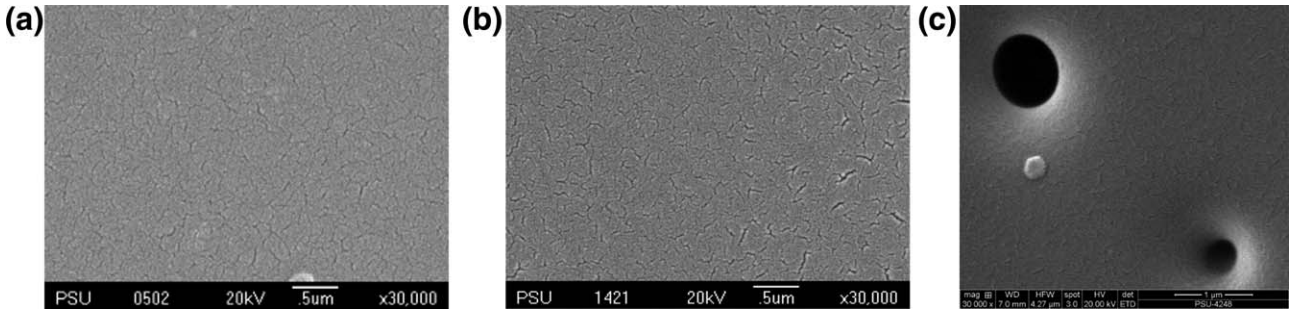

Figure 3. SEM micrographs of the top skin surface of the asymmetric PSF membrane (prepared at CBT 20°C) with an EtOH concentration of (a) 16.4 wt %, (b) 18.4 wt %, and (c) 20.4 wt %.

$$\propto_{ij} = \frac{\left(\frac{P}{l}\right)_i}{\left(\frac{P}{l}\right)_j} = \frac{P_i}{P_j} \quad (2)$$

where P_i and P_j are the permeability of i and j gases, respectively. A schematic diagram of the gas permeation testing set is shown in Figure 2. In this test, the permeate gas was selected through a four-way selective valve and the feed side pressure was controlled by a regulator. The flow rate of the permeate gas through the soap bubble flow meter was recorded when it reached an almost constant value. To compare the gas permeation of each membrane sample the needle valve on the retentate, feed and permeate sides were fixed at the same position. The gas flow rate was read for 5–7 times at each pressure level and the average value is calculated from that.

RESULTS AND DISCUSSIONS

Effect of EtOH Concentration

To study the effect of EtOH concentration, PSF membranes were prepared using a casting solution that consisted of PSF of 22 wt %. In this section, DMAC and THF were utilized as low and high volatile solvents, respectively. The concentration of these two solvents varied with 31.8, 30.8, 29.8, and 28.8 wt %, while the EtOH increased with 14.4, 16.4, 18.4, and 20.4 wt %, respectively. The preparation procedure for this experiment is described in section "Preparation of Asymmetric Flat Sheet Membranes".

Figures 3 and 4 show the top skin surface and cross-section of the produced membranes, respectively. It was found that for a concentration of EtOH in the range of 14.4 to 18.4 wt % a dense skin surface membrane was obtained. Pores were created on the top surface when the concentration of EtOH was about 20.4 wt % as shown in Figure 3(c). In the cross-sectional view, macrovoids appeared in a bulk structure of membranes prepared without EtOH. This macrovoid-structure is vanished and replaced with a sponge-like structure as EtOH was incorporated in the casting solution. The gas permeation testing result also showed that the average CO_2/CH_4 selectivity of asymmetric PSF membranes using EtOH concentrations of 16.4–18.4 wt % was higher than 28.8. However, the CO_2/CH_4 selectivity was lower than 25.4 when the concentration of EtOH in casting solution is 20.4 wt %. This increase of CO_2/CH_4 selectivity is according to the selectivity of membranes reported in the Ref. 13. The ideal CO_2/CH_4 separation factor of membranes prepared with an EtOH concentration of 0, 8, and 14.4 wt % increased from 25.4, over 26.5 to 28.8, respectively. From this result, the ideal separation factor is likely be enhanced by an increase of the EtOH concentration. The discussion of the interaction between higher volatile solvents and non-solvents appeared in the literatures.[1,4,13,15,32]

Effect of Evaporation Time

The experimental results indicated that the ET has an obvious effect to the top skin thickness of PSF membranes. The top skin thickness increased and a few macrovoids appeared in the midst of the sponge-like structures when ET increased. Furthermore, the dense skin surface was formed when ET was increased to 60 s. As illustrated in Figure 5, the skin layer thickness increased to about 8.5 μm when the ET was increased to 60 s. This result is in agreement with results reported in Refs. 16, 32. The

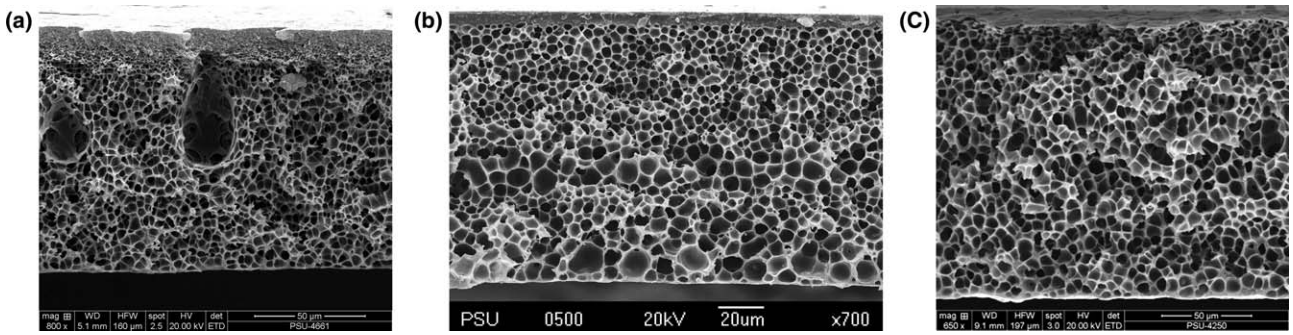

Figure 4. SEM micrographs (×700) of the cross-section of asymmetric PSF membranes (prepared at CBT 20°C) with an EtOH concentration of (a) 0 wt %, (b) 16.4 wt %, and (c) 20.4 wt %.

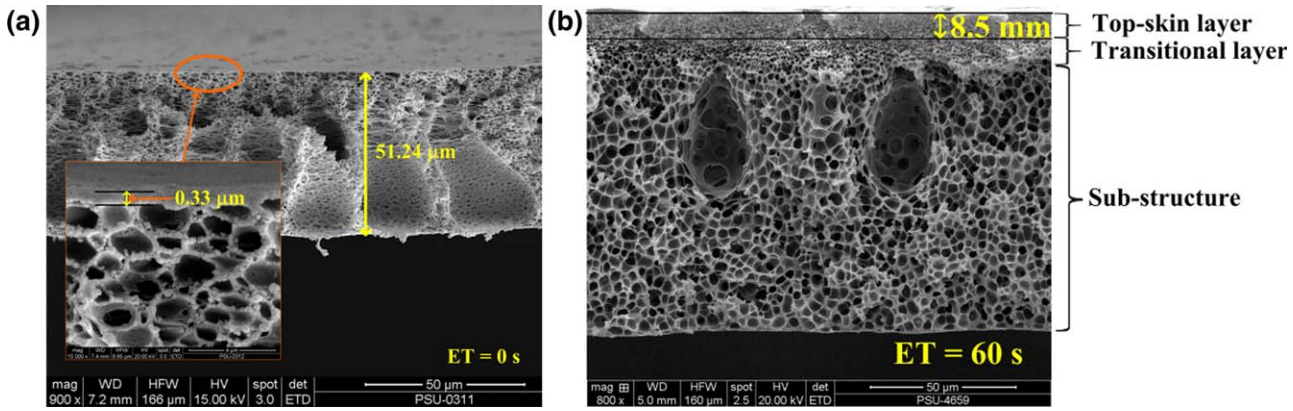

Figure 5. SEM micrographs showing the top-skin thickness of PSF membranes, (a) ET = 0 s and (b) ET = 60 s. [Color figure can be viewed in the online issue, which is available at wileyonlinelibrary.com.]

structure of PSF membrane samples changed when the ET varied from 0 to 40 s. The bi-continuous top surface disappeared and was replaced by a dense skin with a few large pores as the ET increased from 0 to 10 s and 20 s. The dense skin surface with no pores was formed while the ET exceeded 30 s. In addition, the trend of the sponge-like structure increased whereas the finger-like structure or macrovoids decreased with increasing ET.

Effect of Coagulation Bath Temperature

As show in Figure 6(a–d), the CBT has no clear effect on the top skin surface. However, the CBT has an effect on the porosity of PSF membranes as presented in Figure 7(a–d). The largest pore size appeared in the membrane prepared at CBT of 4°C as shown in Table I. This might be an effect from the thermodynamic and kinetic properties of the casting solution. The pore size of PSF membranes prepared at CBT of 10°C is rather

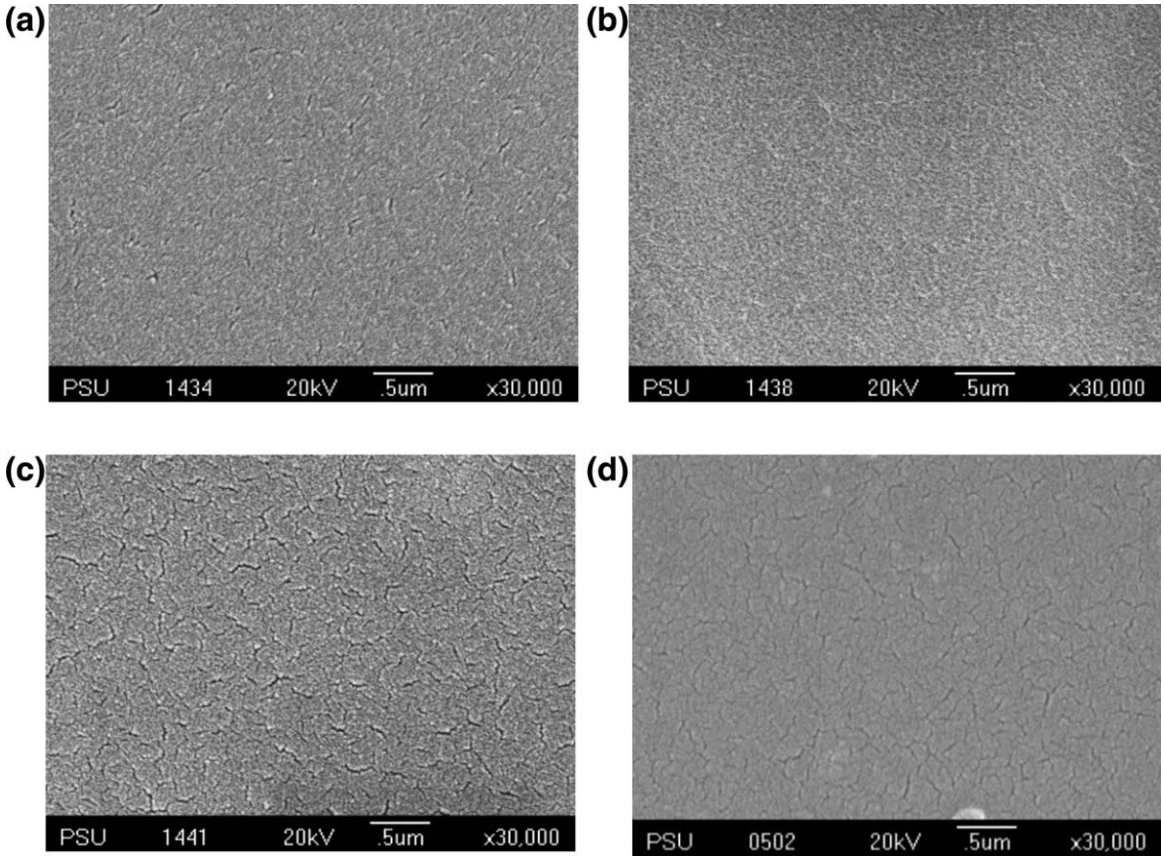

Figure 6. SEM micrographs of the top skin surface of PSF membranes prepared at 16.4 wt % EtOH and CBT varied with (a) 4°C, (b) 10°C, (c) 15°C, and (d) 20°C.

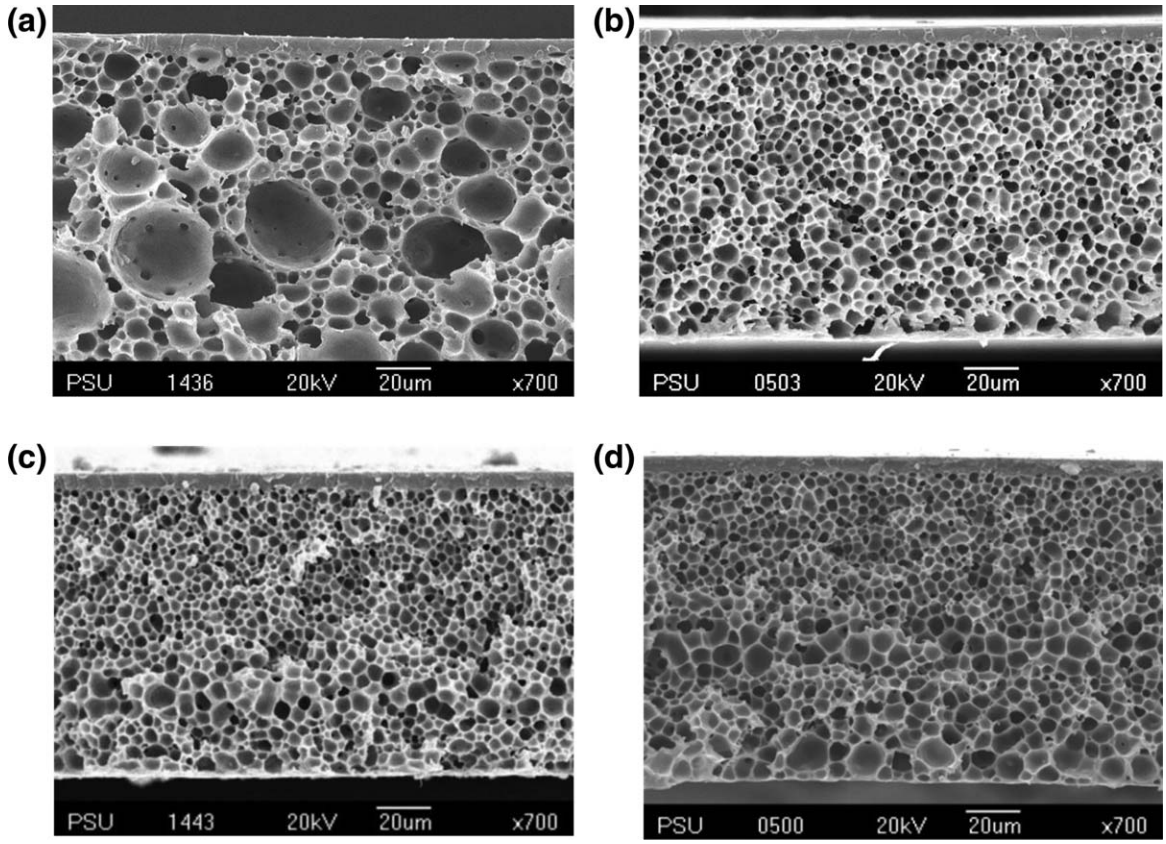

Figure 7. SEM micrographs of the cross section of PSF membranes prepared at 16.4 wt % EtOH and CBT varied with (a) 4°C, (b) 10°C, (c) 15°C, and (d) 20°C.

uniform. However, the pore size varied gradually from the upper to lower part of the membrane cross-section. In addition, the interconnected pore structures were formed in all of the prepared membranes. From the Ref. 13, they reported that the cell diameter increased with an increase of the CBT. Moreover, the membrane thickness and the number of macrovoids increased significantly. For membranes prepared from the casting solution and consisted of 22 wt % PSF, 31.8 wt % DMAc, 31.8 wt % THF, and 14.4 wt % EtOH, the macrovoids were completely removed when the nascent membrane was coagulated at a CBT of 5°C. In the present study, the pore size of the membranes prepared from the casting solution consisted of 22 wt % PSF, 30.8 wt % DMAc, 30.8 wt % THF, and 16.4 wt % EtOH, increased with increasing CBT from 10 to 20°C. Simultaneously, the membrane thickness increased. These results are in good agreement with the results given in Ref. 13 except for the membrane prepared at a CBT of 4°C. Possible reasons here might be the EtOH concentration or the ratio of solvent to nonsolvent (S : SN). Additionally, the preparation procedure was slightly different.

Effect of Plasma Treatment on the Morphology and Structure of PSF Membranes

AFM images of 55 × 55 μm scanned regions of PSF membranes surfaces are presented in Figure 8(a–e). Figure 8(a) shows the surface morphology of an untreated PSF membrane. Figure 8(b–e) illustrate the morphology of PSF membranes after treated with Ar, air, O_2, and CO_2 plasmas at a discharge power of 15 W and exposure time of 5 min. The surface morphology appeared to be different after treated with plasma from different plasma gases. This change is observed through different levels of surface roughness. As the average surface roughness of untreated membrane is about 6.12 nm, the roughness of treated membranes is about 5.49, 11.66, 4.02, and 3.37 nm for Ar, air, O_2, and CO_2 plasmas, respectively. For CO_2-plasma, the surface roughness decreased according to the result reported in Ref. 8.

Figure 9 shows that the water contact angle and the dispersive component decreased while the surface energy and its polar component increased after plasma treatment. At the same conditions, the surface energy of PSF membranes treated with Ar-discharge is the highest. The surface energy related to the hydrophilic property. That is the hydrophilic property increased

Table I. Mean and Max Pore Size of PSF Membranes at Different CBT

CBT (°C)	Mean/Max pore size (μm)
4	5.01/32.87
10	2.42/11.77
15	3.56/12.62
20	3.58/14.91

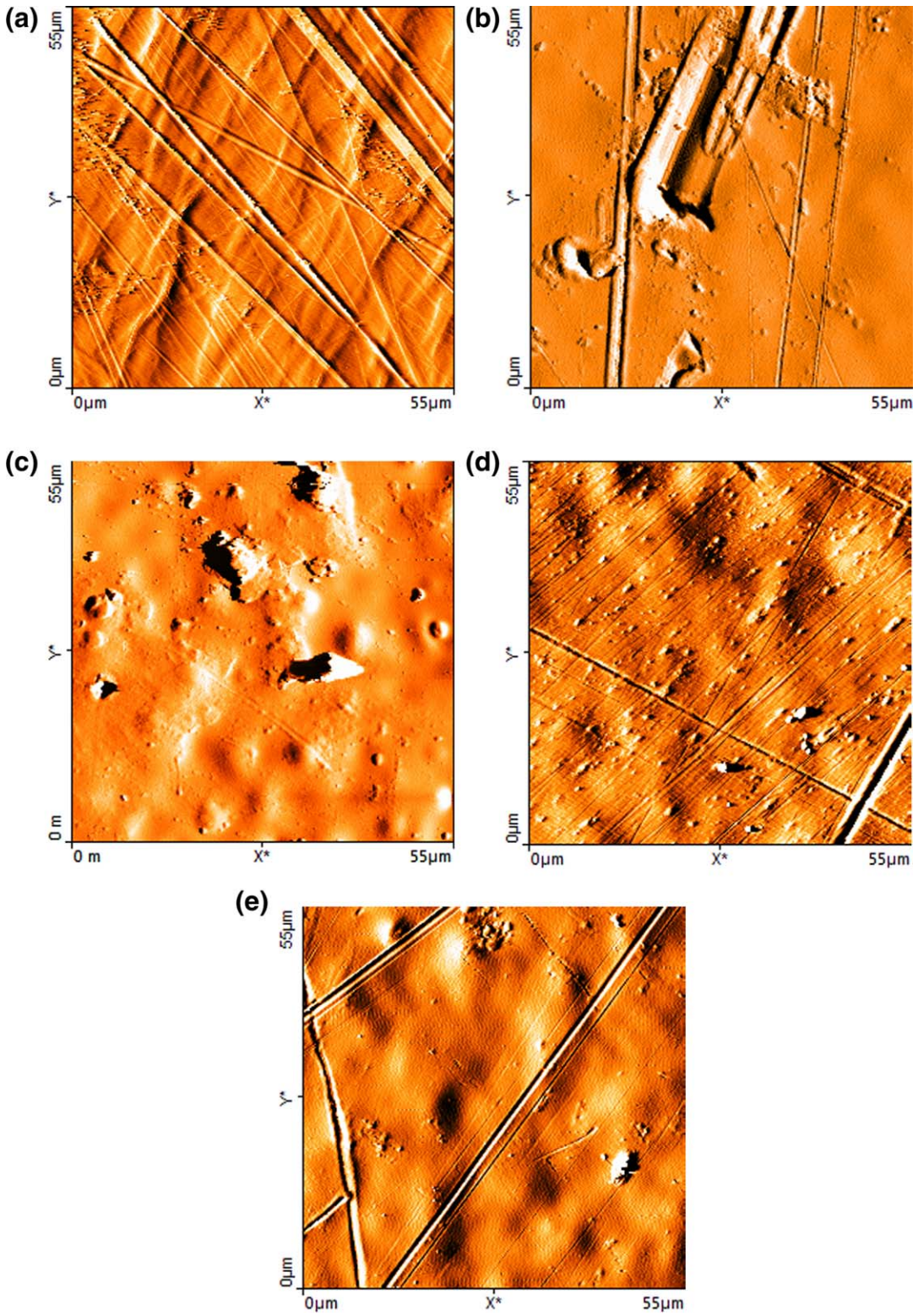

Figure 8. AFM images of PSF membrane surfaces treated with DC-plasma from untreated (a) Ar, (b) Air, (c) O_2, (d) and CO_2 (e) gases at a discharge power of 15 W and a treatment time of 5 min. [Color figure can be viewed in the online issue, which is available at wileyonlinelibrary.com.]

when surface energy is increased. Consequently, the discharge plasma from Ar might be effective in improving the hydrophilic property of PSF membranes.

The results of DMTA investigations show that the glass transition temperature (T_g) of plasma treated PSF membranes as illustrated in Figure 10 exhibits a small shift from about

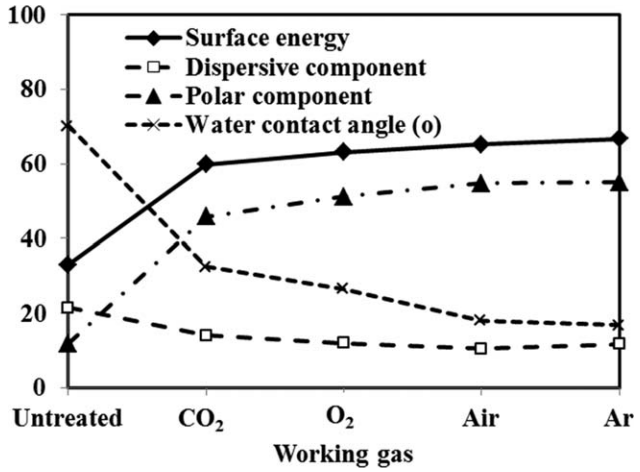

Figure 9. Change of water contact angle and surface energy and its components after treated with the plasma from four working gases.

207.5°C for untreated membranes to about 208.5, 210.0, 206.5, 209.0, and 209.5°C for Ar, N_2, air, O_2, and CO_2 discharge plasmas, respectively. Further, the plasma from all working gases influenced the viscoelasticity of PSF membranes; both the storage and loss modulus declined in all plasma treated membranes. The largest decrease of these two moduli can be observed when the PSF membranes are treated with O_2-plasma.

Effect of Plasma Treatment on Gas Separation Properties of PSF Membranes

In this current work, only the asymmetric PSF membranes, which were prepared from a casting solution consisting of PSF 26.0, NMP 28.0, THF 28.0, and EtOH 18.0 wt %, were plasma treated. The results show that the gas permeation rate of CO_2, CH_4, O_2, and N_2 increased after treated with DC-glow discharge plasma from all working gases, whereas the ideal selectivity of CO_2/CH_4 and O_2/N_2 has receded.

The results from the permeation test of the 15 PSF membrane samples revealed that the permeability of CO_2 through the membranes at a pressure of 5 bars is about 1.56 GPU. For the permeation at this pressure of CH_4 gas, we found that the CH_4 is not permeated through the 14 membrane samples. The permeability of CH_4 through one of 15 samples is about 0.02 GPU as shown in Figure 11(a). The permeability of O_2 and N_2 gases at 5 bars were calculated from the permeation rate. The N_2 did

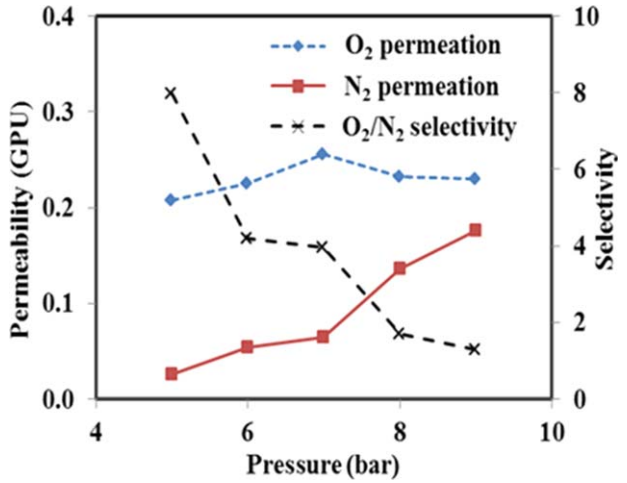

Figure 11. Permeation of CO_2, CH_4, O_2, and N_2 and selectivity of CO_2/CH_4 and O_2/N_2 at different pressure levels. [Color figure can be viewed in the online issue, which is available at wileyonlinelibrary.com.]

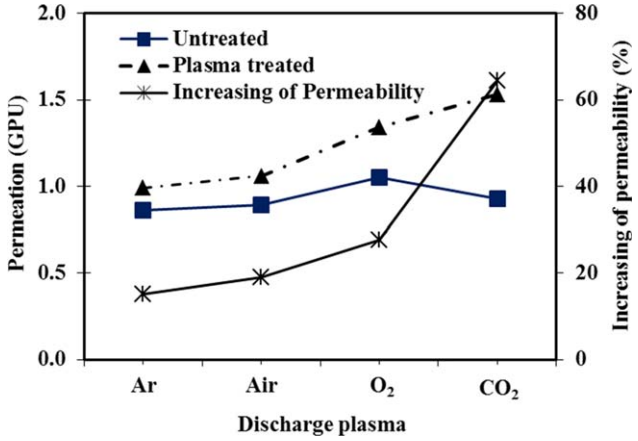

Figure 12. Comparison of CO_2 permeation through untreated and plasma treated PSF membranes. [Color figure can be viewed in the online issue, which is available at wileyonlinelibrary.com.]

not permeate through the membrane except it was fed with a pressure of 6, 7, 8, and 9 bars. In contrast, the O_2 can permeate at pressure levels of 5–9 bars. The maximum CO_2/CH_4 and O_2/N_2 selectivity of untreated membranes at a pressure of 5 bars was about 69.76 and 12.59, respectively. The average O_2/N_2

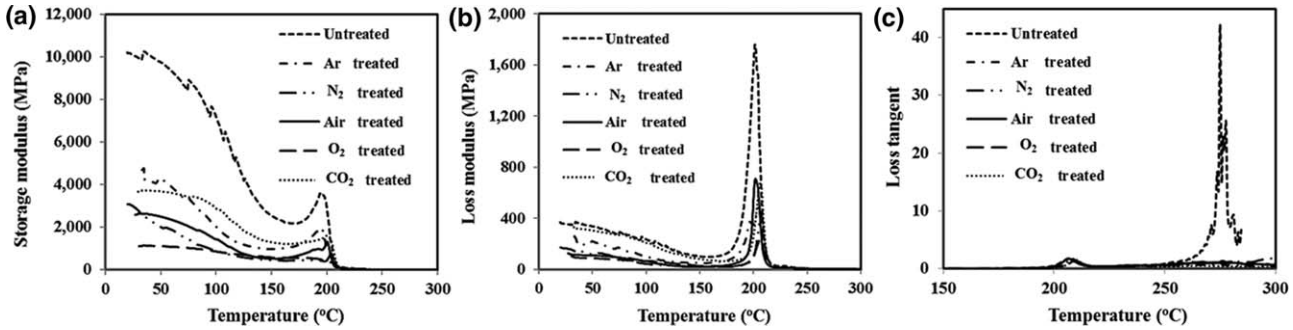

Figure 10. (a) Change of storage modulus, (b) loss modulus, and (c) loss tangent or *tanδ* with temperature.

selectivity through untreated membranes at different pressures is illustrated in Figure 11(b). It is clear that the selectivity decreased as the pressure increased from 5 to 9 bars.

For plasma treated membranes, the selectivity values of the gases tend to be lower; however, the CO_2/CH_4 selectivity is still higher than 40.41 for O_2-treated plasma as reported in Ref. 3. In contrast, the permeation of all gases through all membranes increased significantly as shown in Figure 12. For example, the permeability of CO_2 increased from about 0.89, 1.05, 0.86, and 0.93 GPU to 1.06, 1.34, 0.99, and 1.53 GPU after treated with air, O_2, Ar, and CO_2 plasmas, respectively. The increase of CO_2 permeation is highest among these four working gases. This might be caused from the etching process that occurred when the nonpolymerizing gas is utilized as a discharge plasma media. According to the difference of the physicochemical properties of these working gases, the gas permeation rates through the plasma treated membranes varied after treated with the discharge plasma from different working gases.

CONCLUSIONS

The conclusion of this study can be divided into two parts. First, the preparation of flat sheet asymmetric PSF membranes by dry-wet phase inversion technique cooperated with the double coagulation bath method. By the variation of the ET, EtOH concentration, and CBT, an asymmetric PSF membrane can be obtained. The skin thickness increases with an increase of ET. Asymmetric PSF membranes with defect-free and dense skin layer were produced when the EtOH concentration was less than 20.4 wt %. The CBT affected the pore size and pore distribution of PSF membranes. The O_2/N_2 selectivity at a pressure of 8 bars of a membrane prepared with an EtOH concentration of 14.4, 16.4, 18.4, and 20.4 wt % is about 14.77, 6.01, 3.27, and 4.11, respectively. The ET has an effect to the thickness of the top skin layer, while the CBT has an influence on the morphology of the obtained membranes; the porosity and pore size tend to increase when the CBT is down to 4°C. The pore structure of the membrane prepared at a CBT of 10°C is quite uniformed.

The second conclusion is about the effects of DC plasma from different working gases. The results show that the plasma from all working gases has an effect on the modulus, viscoelasticity, and the glass transition temperature of plasma treated membranes. The modulus of plasma treated membranes decreased. The largest decrease of modulus occurred after O_2-plasma treatment. Furthermore, the gas permeability of plasma treated membranes increased as the selectivity of CO_2/CH_4 and O_2/N_2 decreased significantly. However, the CO_2/CH_4 selectivity of asymmetric PSF membranes prepared from a casting solution consisted of PSF 26 wt %, NMP 28 wt %, THF 28 wt %, and EtOH 18 wt % incorporated with the elaborated process is higher than that is reported in elsewhere.[13,31]

ACKNOWLEDGMENTS

Financial supported from the Thailand Center of Excellence in Physics (ThEP) through a fellowships program are acknowledged. The authors wish to thank the Department of Physics and the Membrane Science and Technology Research Center (MSTRC), both Prince of Songkla University (PSU), for supporting work places, devices, and materials.

REFERENCES

1. Guillen, G. R.; Pan, Y.; Li, M.; Hoek, E. M. V. *Ind. Eng. Chem. Res.* **2011**, *50*, 3798.
2. Castro Vidaurre, E. F.; Achete, C. A.; Gallo, F.; Garcia, D.; Simão, R.; Habert, A. C. *Mater. Res.* **2002**, *5*, 37.
3. Modarresi, S.; Soltanieh, M.; Mousavi, S. A.; Shabani, I. *J. Appl. Polym. Sci.* **2012**, *124*, E199.
4. Madaeni, S. S.; Moradi, P. *J. Appl. Polym. Sci.* **2011**, *121*, 2157.
5. Navaneetha Pandiyaraj, K.; Selvarajan, V.; Deshmukh, R. R.; Bousmina, M. *Surf. Coat. Technol.* **2008**, *202*, 4218.
6. Martin, P. M. Handbook of Deposition Technologies for Films and Coatings: Science, Application and Technology, 3rd ed.; Elsevier: USA. ISBN-13:978-0-8155-2031-3, **2010**.
7. Pierson, H. O. Handbook of Chemical Vapor Deposition: Principles, Technology and Applications 2nd ed.; Noyes Publications/William Andrew Publishing, LLC Norwich: New York. ISBN: 0-8155-1432-8, **1999**.
8. Baruah, K.; Hazarika, S.; Borthakur, S.; Dutta, N. N. *J. Appl. Polym. Sci.* **2012**, *125*, 3888.
9. Yuenyao, C.; Chittrakarn, T.; Tirawanichakul, Y.; Saeung, P.; Taweepreda, W. *Thai J. Phys.* **2012**, *8*, 41.
10. Ismail, A. F.; Lai, P. Y. *Sep. Purif. Technol.* **2004**, *40*, 191.
11. Ma, Y.; Shi, F.; Ma, J.; Wu, M.; Zhang, J.; Gao, C. *Desalination* **2011**, *272*, 51.
12. Aroon, M. A.; Ismail, A. F.; Montazer-Rahmati, M. M.; Matsuura, T. *Sep. Purif. Technol.* **2010**, *72*, 194.
13. Pakizeh, M.; Mansoori, S. A. A.; Pourafshari Chenar, M.; Namvar-Mahboub, M. *Braz. J. Chem. Eng.* **2013**, *30*, 345.
14. Han, M. J.; Nam, S. T. *J. Membr. Sci.* **2002**, *202*, 55.
15. Pesek, S. C.; Koros, W. J. *J. Membr. Sci.* **1993**, *81*, 71.
16. Ismail, A. F.; Norida, R.; Abdul Rahman, W. A. W.; Matsuura, T.; Hashemifard, S. A. *Desalination* **2011**, *273*, 93.
17. Yamasaki, A.; Tyagi, R. K.; Fouda, A. E.; Matsuura, T.; Jonasson, K. *J. Appl. Polym. Sci.* **1999**, *71*, 1367.
18. Vandencasteele, N.; Reniers, F. *J. Electron. Spectrosc. Relat. Phenom.* **2010**, *178–179*, 394.
19. Wavhal, D. S.; Fisher, E. R. *Desalination* **2005**, *172*, 189.
20. Hopkins, J.; Badyal, J. P. S. *Langmuir* **1996**, *12*, 3666.
21. Pal, S.; Ghatak, S. K.; De, S.; DasGupta, S. *J. Membr. Sci.* **2008**, *323*, 1.
22. Kim, K. S.; Lee, K. H.; Cho, K.; Park, C. E. *J. Membr. Sci.* **2002**, *199*, 135.
23. Gancarz, I.; Poźniak, G.; Bryjak, M. *Eur. Polym. J.* **1999**, *35*, 1419.

24. Gancarz, I.; Poźniak, G.; Bryjak, M. *Eur. Polym. J.* **2000**, *36*, 1563.
25. Švorčík, V.; Kolářova, K.; Slepička, P.; Macková, A.; Novotná, M.; Hnatovicz, V. *Polym. Degrad. Stab.* **2006**, *91*, 1219.
26. Jian, C.; Jiding, L.; Cuixian, C. *Plasma Sci. Technol.* **2009**, *11*, 42.
27. Akishev, Y.; Grushin, M.; Dyatko, N.; Kochetov, I.; Napartovich, A.; Trushkin, N.; Minh Duc, T.; Descours, S. *J. Phys. D: Appl. Phys.* **2008**, *41*, 1.
28. Hejda, F.; Solar, P.; Kousal, J. WDS'10 Proceedings of Contributed Papers, Part III, **2010**; pp 25–30.
29. Schols, P. Carnoy 2.0. Laboratory of Plant Systematics. Katholieke Universiteit Leuven: Flanders, Belgium, **2001**, http://www.kuleuven.ac.be/bio/sys/carnoy.
30. Scholes, C. A.; Kintish, S. E.; Stevens, G. W. *Recent Pat. Chem. Eng.* **2008**, *1*, 52.
31. Baker, R. W. Membrane Technology and Applications, 2nd ed.; Wiley: UK. **2004**, pp 303–305.
32. Peng, Y.; Dong, Y.; Fan, H.; Chen, P.; Li, Z.; Jiang, Q. *Desalination* **2013**, *316*, 53.
33. Shilton, S. J.; Ismail, A. F.; Gough, P. J.; Dunkin, I. R.; Gallivan, S. L. *Polymer* **1997**, *38*, 2215.